ARTICLE

Highly crosslinked, chlorine tolerant polymer network entwined graphene oxide membrane for water desalination

Received 00th January 20xx,
Accepted 00th January 20xx

DOI: 10.1039/x0xx00000x

www.rsc.org/

Seungju Kim[a], Xiaocheng Lin[a], Ranwen Ou[a], Huiyuan Liu[a], Xiwang Zhang[a], George P. Simon[b], Christopher D. Easton[c], and Huanting Wang[*a]

Graphene and its derivatives are very attractive for constructing membranes for high-efficiency separation applications including water purification and desalination. To develop practical desalination membranes, strictly controlled inter-layer distance of graphene-based laminates and strong adhesion of graphene-based selective layer onto a porous polymer substrate are required to provide high salt rejection properties and desirable mechanical durability with chlorine tolerance in the membrane processes. However, there is a difficulty in stabilizing graphene nanosheets as a membrane selective layer for desalination process and controlling interlayer distance. In this work, we demonstrate the successful fabrication of graphene-based thin-film composite membrane by integrating graphene oxide (GO) nanosheets into a highly crosslinked polymer network on a porous polymer substrate. The resulting poly(N-isopropylacrylamide-co-N,N'-methylene-bisacrylamide) entwined GO thin-film composite membrane has a main GO interlayer spacing of 0.48 nm and a GO-polymer thin film of less than 40 nm thick, and shows excellent water flux (25.8 L m^{-1} h^{-1}) and salt rejection (a NaCl rejection of 99.9%), alongside excellent mechanical stability and chlorine tolerance for the forward osmosis process. This polymer network entwined GO thin-film composite can be effectively tailored as a platform material for developing high-performance osmosis desalination membranes for industrial application.

Introduction

Membrane-based separation represents a simple and effective process in many industrial separation applications such as water purification and desalination because of their advantages over other separation processes in terms of energy savings and low cost.[1-6] In particular, membrane water desalination and purification by the reverse osmosis (RO) process has dominated over 60% desalination capacity in the world and the osmotic pressure-driven processes such as forward osmosis (FO) and pressure-retarded osmosis (PRO) processes have developed as a potential alternative to RO process in wastewater treatment, seawater desalination, and energy production.[6-11]

Polyamide (PA) has been the main membrane material for membrane desalination with its high water flux and salt rejection, and PA membrane is commonly used as RO or nanofiltration in the stage of water desalination processes, and recently being developed for application. However, the major drawback of PA is their poor stability against oxidizing agents such as chlorine which is commonly used in water desalination and purification to kill microorganisms and minimize membrane biofouling. Therefore, in industrial membrane desalination processes, apart from large suspended particles being removed in the pre-treatment, the feed water is chlorinated first and then dechlorinated before being passed through the RO membrane modules for desalination. The water is finally rechlorinated to maintain its freshness and be sent to water supply network. Hence, the poor oxidation stability of polyamide membrane leads to extra dechlorination-rechlorination steps and adds significant costs in water industry.[12] Therefore, the development of chlorine-resistant osmosis membrane is of significant interest for various industries involving desalination processes in terms of reducing the membrane process complexity and the costs of water processing.[13-15]

Graphene-based materials have been of great interest for many potential membrane-based separation applications such as ion separation, gas separation, water purification and desalination.[16-22] Recent years have seen tremendous research efforts in the development of graphene-based membranes from either holey graphene nanosheets, graphene oxide or reduced graphene oxide laminates.[23-26] Because of its atomic thickness, robustness and potential for functionalization, graphene and its derivatives have been considered as attractive building blocks to construct high-performance separation membranes. As individual graphene nanosheets are known to be inherently impermeable to all molecules, graphene-based membranes are mainly fabricated by

[a] Department of Chemical Engineering, Monash University, VIC 3800, Australia. E-mail: huanting.wang@monash.edu
[b] Department of Materials Science and Engineering, Monash University, VIC 3800, Australia.
[c] CSIRO Manufacturing, Bayview Ave, Clayton, VIC 3168, Australia.

† Footnotes relating to the title and/or authors should appear here.
Electronic Supplementary Information (ESI) available: [details of any supplementary information available should be included here]. See DOI: 10.1039/x0xx00000x

producing either nanoporous graphene (also known as holey graphene) or graphene oxide (GO)/reduced graphene oxide (rGO) laminates.[23-29] Molecular dynamics simulation study showed that porous graphene had great potential for water desalination,[29] and a number of techniques such as chemical oxidation or air oxidation have been developed to prepare holey graphene,[24, 26-28] but the large-scale and cost-effective fabrication of such holey graphene-based ultrathin membranes with desired salt rejection remains a great challenge. By contrast, GO or rGO laminate membranes can be easily prepared by filtration or coating of GO nanosheet suspensions.

It is well known that the mass transport through GO/rGO membranes mainly relies on interlayered nanochannels.[30] When GO laminate membranes are immersed in water and become hydrated, they show excellent ionic sieving properties for small hydrated ions such as K^+, AsO_4^{3-}, or Mg^{2+}.[17] GO/rGO membranes also perform nanofiltration membranes, showing good rejection of dye molecules.[31, 32] By incorporating hydrophilic thermo-responsive polymer into GO interlayers, the resulting GO nanocomposite membrane shows temperature-responsive changes in water flux and rejection in the nanofiltration processes.[33] GO laminates were also assembled on PA surface with physical interaction and chemical reaction such as via poly(tannic acid) crosslinking to enhance antimicrobial effect and slow down PA degradation by oxidizing agent in water treatment processes.[34-38] GO/rGO laminate membranes and their polymer composite membranes have a potential to apply for desalination processes.[2, 5-7, 39]

The remarkable separation properties of GO/rGO laminate membranes could bring high water flux and salt rejection for desalination process. Moreover, chemically stable GO could be beneficial in the chlorine degradation issues of commercially available and widely used CTA and PA membranes in water treatment processes.[12-14] However, GO/rGO laminate membranes and their polymer composite membranes reported so far have either low salt rejection or poor structural stability and mechanical strength, and thus they are not suitable for practical desalination applications. More importantly, structural weakness of GO/rGO membranes in aqueous conditions would bring difficulty of long-term water treatment operations. Immobilization of GO by chemical reaction with polymer or organic molecules has been studied for nanofiltration and seawater desalination to improve performance of GO membranes.[40-42] The GO/rGO membranes reported so far are prepared by simple and facile vacuum assisted filtration method from an aqueous solution,[17] however, ultrathin GO/rGO membranes are easily re-dispersed into water during water-based operations. As a result, GO/rGO membranes have difficulty of controlling interlayer distance and reducing selective layer thickness for practical industrial applications.

Herein we report on mechanically robust, chlorine-tolerant polymer network entwined GO composite membranes for energy-efficient forward osmosis desalination. As schematically illustrated in **Fig. 1**, the membranes are composed of an ultrathin GO-polymer layer with a thickness of less than 40 nm supported on a porous polymer membrane substrate. The GO-polymer layer is prepared by spin-coating of GO-organic monomer solution on the substrate to form a layer of GO scaffold filled up with the monomer solution, followed by polymerization of monomers. The mixture of monomers contains a high proportion of bifunctional monomer and the remaining monofunctional monomer, so a highly crosslinked, dense polymer network is produced to wrap up GO nanosheets together. Such an ultrathin highly crosslinked polymer network entwined GO layer is mechanically-strong and chemically-durable and enables both high water flux and salt rejection, thus providing a platform material for developing desalination membranes. In principle, by choosing the appropriate type of porous polymer substrate (high mechanical strength for RO and high porosity for FO desalination applications), the polymer network entwined GO can be made into both RO and FO membranes. To demonstrate the FO membrane fabrication process, monofunctional N-isopropylacrylamide (NIPAM) and difunctional N,N'-methylenebis(acrylamide) (MBA) are used as monomers, and ammonium persulfate (APS) is used an initiator in this study. Highly crosslinked poly(NIPAM-MBA) network is formed on a highly porous polymer substrate by free radical polymerization of NIPAM and MBA, which is initiated by thermal composition of APS.

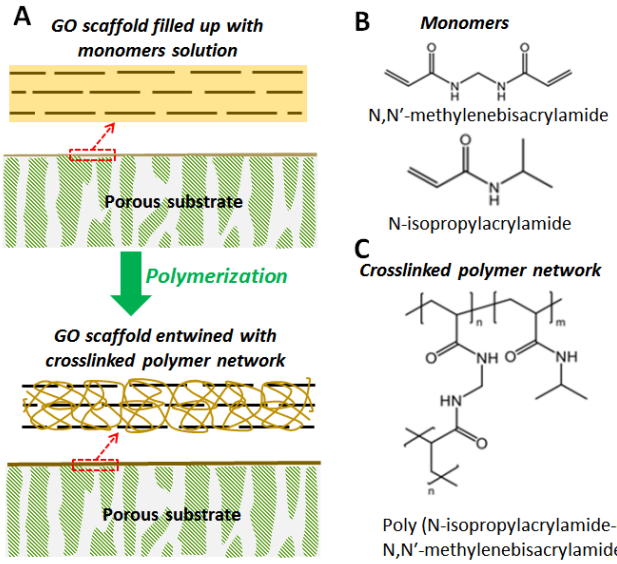

Fig. 1 (A) Schematic diagram of the fabrication of a GO-polymer network composite membrane for forward osmosis desalination. A thin layer of GO scaffold filled up with monomers solution is formed on a porous polymer substrate via spin coating, followed by free radical polymerization of monomers. (B) Molecular structure of monomers, N,N'-methylenebisacrylamide and N-isopropylacrylamide. (C) Highly crosslinked polymer network formed in the composite membrane.

Experimental

Fabrication of GO-polymer membrane. Graphene oxide was synthesized from graphite powder by modified Hummers

method. The concentration of the resulting GO suspension was 3.8 mg/ml in water.[43, 44] The GO concentration was determined by freeze-drying of 10 ml GO suspension, and weighing the residual solid (GO). Monomers to fabricate a polymer network within GO laminate scaffold including N-isopropylacrylamide (NIPAM), N,N'-methylenebisacrylamide (MBA), and ammonium persulfate (APS) were purchased from Sigma-Aldrich (St Louis, MO) and used without further purification. Specifically, 38 mg of NIPAM, 38 mg of MBA, and 7 mg of APS were dissolved into 10 ml GO suspension. To vary the ratio of GO/poly(NIPAM-MBA) from 4.5 to 50%, the same amounts of NIPAM, MBA and APS were added into 10 ml GO suspension with a different GO loading, 3.4, 4.8, 9.5, 19, 28.5, and 38 mg. Note that the GO suspension with a different GO loading was obtained by diluting 3.8 mg/ml GO suspension. Detailed quantities of components in the preparation are summarized in **Table S1**.

Precursor solution including GO and monomers was sonicated for 30 minutes to completely dissolve. Nylon membrane substrate, obtained from Sterlitech Corporation (product number NY4547100, Kent, WA, USA), was used as a support layer with a diameter of 47 mm and average pore size of 450 nm. Nylon substrate was floated on 10 ml of precursor solution in a glass petri dish for 30 seconds, set on a spin-coater (WS-650-23B, Laurell Technologies Corporation, PA, USA), and spun for 30 seconds in 1,000 rpm, then located in a convection oven (Thermal Fisher) at 70 °C for 2 h for complete free-radical polymerization of monomers.[45-47] Coating and polymerization procedures were repeated for 3 times to ensure the formation of a defect-free GO-polymer composite layer on the Nylon substrate.

Characterization. The morphology of GO-polymer membranes was observed using a field emission scanning electron microscope (FE-SEM) (Nova NanoSEM 450, FEI, Hillsboro, OR). Atomic force microscopy (AFM) images of the surfaces of the GO-polymer membrane and the layered GO membrane were taken in tapping mode using a Bruker Dimension Icon microscope (Bruker, Billerica, MA, USA). Chemical structure of the GO-polymer membrane was analyzed by Fourier transform infrared spectroscopy, and the spectrum was obtained from the membrane surface using a Attenuated total reflectance-Fourier transform infrared spectroscopy (ATR-FTIR) instrument (Perkin Elmer, Spectrum 100). The crystalline structure of membrane samples was determined by X-ray diffraction technique (XRD, Miniflex 600 X-ray diffractometer, Rigaku, Japan). X-ray photoelectron spectroscopy (XPS) analysis was performed using an AXIS Nova spectrometer (Kratos Analytical Inc., Manchester, UK) with a monochromated Al Kα source at a power of 180 W (15 kV x 12 mA) and a hemispherical analyser operating in the fixed analyser transmission mode. For comparison, layered GO membrane was prepared by spin-coating of a dilute GO solution (1.0 mg/ml) on the Nylon substrate with the same method for GO-polymer membrane fabrication. Thermogravimetric analysis (TGA) of GO-polymers was performed to determine GO and polymer compositions, where precursors were spin-coated on the glass plate and heat-treated with the same procedure; after 10 times repetitive steps to obtain an sufficient amount of samples for TGA, around 50 mg of GO-polymer composite was scraped off from the glass plate by a sharp knife, and TGA was performed in nitrogen atmosphere with 10 °C/min ramping rate.

Forward osmosis (FO) performance measurement. Water flux and reverse salt flux of GO-polymer membranes and commercial CTA membranes obtained from HTI in FO process were measured at room temperature using a laboratory scale FO testing system which was assembled with components (Natural acetal copolymer (Delrin) Cell #CF042D-FO and FO Carboy Tank Pump #1220189) purchased from Sterlitech (Kent, WA, USA). The effective area of 0.2 cm^2 was loaded into the cell, and both feed and draw solution cross-flow rates were set at 500 cm^3/min. Deionized water or 2,000 ppm NaCl aqueous solution was used as feed solution, and a NaCl aqueous solution with a concentration ranging from 0.5 M to 2.0 M was used as draw solution. The FO performance of GO-polymer membrane was determined in both FO and PRO modes. The feed and draw solution tanks were weighed continuously using two digital balances connected to a computer. The water flux of the membrane was calculated from the weight changes of the feed and draw solutions. The electrical conductivity of the feed and draw solutions was measured to determine the salt concentration of the feed and draw solutions, which was used to calculate the reverse salt flux. Three samples of each membrane were measured. The calculations of the water flux, reverse salt flux and salt rejection were detailed in the supplementary information.

Chlorine tolerance characterization. Chlorine tolerance of GO-polymer membranes was evaluated using aqueous solutions of sodium hypochlorite (NaOCl) at concentrations of 100 and 1,000 ppm. Before chlorine exposure, the water flux and reverse salt flux of the GO-polymer membrane were measured as described the above section. The GO-polymer membrane was then immersed in the NaOCl solution and kept for 24 h at room temperature. Then the membrane was taken out and completely washed with deionzied water remove residual NaOCl solution. The water flux and reverse salt flux were measured again. The changes in water flux and reverse salt flux before and after chlorine exposure were compared to determine membrane chlorine stability. For comparison, cellulose triacetate FO) membranes with an embedded polyester screen mesh (Hydration Technologies Inc., Albany, OR, USA were tested before and after chlorine exposure under the similar conditions. Three samples of each membrane were tested.

Results and discussion

Polymer network entwined GO membranes were fabricated to demonstrate their high performance in FO water desalination process. The highly porous Nylon membrane was chosen as a substrate to provide mechanical support while minimizing

internal concentration polarization that is a key problem for FO process. The random copolymer, poly(*N*-isopropylacrylamide-*co*-*N,N*'-methylene-bis-acrylamide) (or poly(NIPAM-MBA)), was produced by free radical polymerization of NIPAM and MBA monomers via opening of C=C double bond.[45-47] Poly(NIPAM-MBA) is densely crosslinked and hydrophilic, and firmly becomes entwined around GO laminate scaffold on the Nylon substrate, allowing water permeation and rejecting hydrated ions. Importantly this poly (NIPAM-MBA) polymer network is highly stable in chlorinated water and mechanically robust for membrane fabrication and operation.

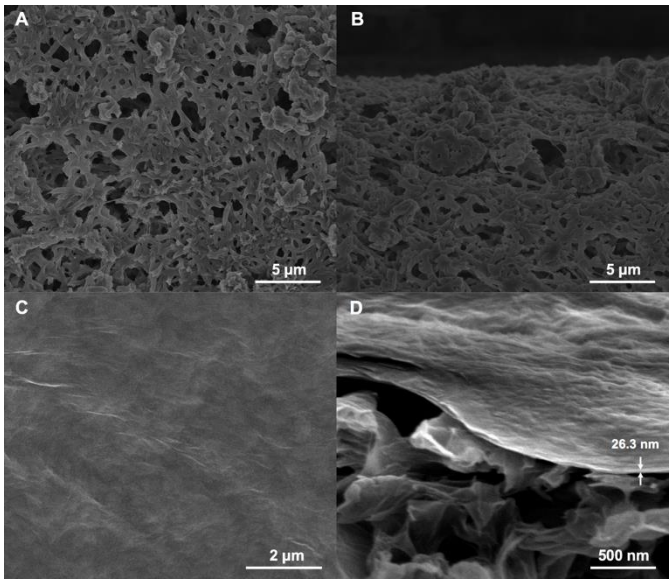

Fig. 2 SEM images of Nylon support: (A) surface, (B) cross section; and GO-polymer composite membrane (GO-P61); (C) sur-face, and (D) cross section.

Table 1 Actual GO contents in GO-polymers after spin-coating

Samples	GO/poly(NIPAM-MBA) weight ratio (%)	
	In solution (GO/monomers)	In membrane (GO/polymer)
GO-P61	4.5	60.7
GO-P65	6.3	65.2
GO-P72	12.5	71.5
GO-P79	25.0	78.7
GO-P87	37.5	87.0
GO-P95	50.0	95.1

As illustrated in **Fig. S1** and **Fig. S2**, the GO- poly(NIPAM-MBA) thin selective layer was prepared by spin coating and subsequent polymerization and drying. The mass ratio of GO and monomers in the precursor solution was varied from 4.5 to 50.0 wt% GO to investigate the effects of membrane composition on the water flux and rejection of the membrane. During the spin-coating, different proportions of the monomer solution and GO nanosheets were lost under centrifugal force due to molecular size and structure. Micro-sized GO nanosheets assembled into a laminate scaffold on the Nylon substrate, where a significant amount of monomers was lost with water during the spin coating and the remained monomer solution was confined within GO interlayer spaces. Consequently, the ratio of GO/poly(NIPAM-MBA) changed after the spin-coating. It is worth mentioning that without GO nanosheets, all of the monomer solution was lost whilst being spin-coated, and no coating was formed. To determine the actual GO content in the GO-polymer layer, thermogravimetric analysis (TGA) was conducted (**Fig. S3**), and the GO weight percentage was calculated on the basis of relative weight loss of polymer and GO. The actual GO amount ranged from 60.7 to 95.1 wt%, as summarized in **Table 1**.

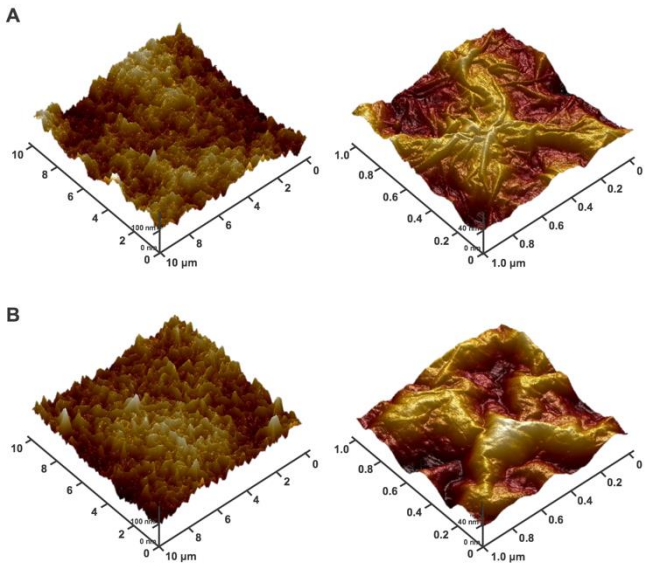

Fig. 3 3D AFM images of (A) a GO-polymer composite membrane (GO-P61) and (B) a layered GO membrane prepared by spin-coating.

As shown in **Fig. 2**, the commercial Nylon membrane substrate exhibited a high porosity and rough surface. Uniform GO-polymer membrane without visible defects was successfully fabricated onto this substrate as confirmed by the SEM images (**Fig. 2**). The GO-polymer layer thickness can be seen from the cross-sectional SEM image to be about 26.3 nm. It is clear that GO nanosheets thus serve as a scaffold and play a key role in forming such a thin film on the rough substrate surface. During the polymerization process, the monomer solution confined within GO laminate layer, where the polymerization occurred, leading to defect-free nanocomposite membranes from a highly crosslinked polymer network that physically entwined GO nanosheets with a charge interaction between GO and polymer as confirmed by XPS spectra (**Fig. S4**).[48] The chemical structure of the membrane was confirmed by ATR-FTIR (**Fig. S5**). Also there was no evidence that the polymer network had any chemical bonding with GO nanosheets. The surface morphology of polymer network entwined GO layer was characterized by atomic force microscopy (AFM). As described in **Fig. 3** and **Fig. S6**, the GO-polymer membrane shows smoother surface compared to the GO membrane. When AFM images are magnified by ten times, the difference of the height of the ridges of the stacked GO laminates are more evident.

The ridges shown in membranes are the edge of stacked GO laminates. GO membrane, prepared by spin-coating from dilute GO solution, has protruded ridges. However, GO-polymer membrane has lower ridge as GO laminates are covered by polymer networks which makes it relatively more levelled surface. The height of the ridges in GO membrane is roughly 35 nm, whereas that in GO-polymer membrane is about 20 nm. Also, the width of ridges resulting from the stacked GO laminates are much thinner in GO-polymer membrane; the width of ridges in GO membrane is more than 100 nm, whereas GO-polymer membrane shows about 50 nm width of ridges.

Water flux and salt rejection (or reverse salt flux) are two commonly used parameters in characterizing the performance of desalination membranes. In our work, the performance of GO-polymer membranes was evaluated in a FO setup. The driving force for water flow in FO process is the osmotic pressure difference between feed and draw solution, therefore additional hydraulic pressure input is not required. The draw solution such as NaCl, $MgSO_4$, and $MgCl_2$ aqueous solutions, which has greater osmotic pressure than the feed water, was used to generate water flow through a membrane.[7, 49] Typically, in the laboratory scale FO tests, the membrane selective layer faces either feed side (FO mode) or draw solution (PRO, mode).[50] In these two different testing modes, the water flux and reverse salt flux can be different because of internal concentration polarization (ICP) effect. In FO mode, ICP in the porous support layer decreases osmotic pressure of a draw solution, resulting in a lower osmotic pressure difference between feed and draw solution, and thus decreasing water flux. In PRO mode, ICP effect is less severe than that in FO mode because draw solution directly contacts to a membrane selective layer, then it reduces osmotic pressure drop. However, the PRO mode is not practical for industrial FO applications due to fouling problems.[50] In our work, NaCl solution was used as draw solution while deionized water and 2,000 ppm NaCl solution were used as feed.

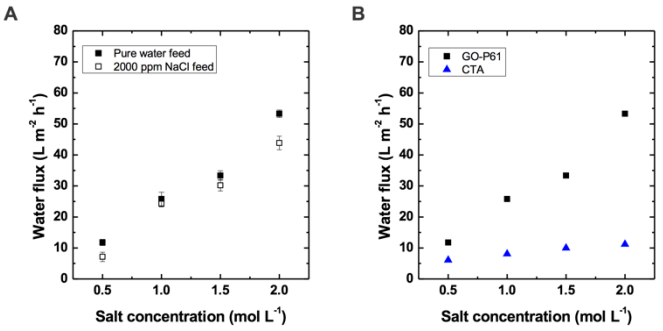

Fig. 4 Water flux of GO-polymer membranes (GO-P61) (A) as a function of various feed and draw salt concentration, and (B) as a comparison with CTA FO membranes.

Fig. 4 shows the FO performance of GO-polymer membranes in terms of water flux, reverse salt flux, and salt rejection as a comparison of other FO membranes reported. Initially, FO performances was investigated with GO-P61 membranes containing 61 wt% GO by polymer network. GO-polymer membranes demonstrated a water flux of 25.8 (L m^{-2} h^{-1}) which is more than 3 times higher compared to the commercial cellulose triacetate (CTA) membrane,[18, 50, 51] as shown in **Fig. 4**. In comparison with the freestanding rGO membranes, GO-polymer composite membranes exhibited similar water flux. However, the GO-polymer membranes are mechanically durable and suitable for practical applications; they maintained similar performance after weeks of FO testing in the lab, indicating that the GO-poly(NIPAM-MBA) selective layer is mechanically strong and has excellent adhesion with the Nylon substrate. By contrast, the freestanding rGO membranes are easily damaged in the circulation of feed water and draw solution during the tests. When 2,000 ppm salt water was used as the feed solution, the water flux of the membrane dropped by 15%. The increase in water flux of commercial CTA gradually declined at high salt concentration, indicating that osmotic pressure difference did not increase to the certain level due to ICP effects, resulting in the self-limiting of water flux at high salt concentration. However, GO-polymer membranes were hardly affected by ICP because a highly porous Nylon substrate was used. Therefore, the water flux difference between GO-polymer membrane and CTA membrane became larger at high salt concentrations. Water flux of GO-polymer membranes demonstrated almost a linear tendency as a function of draw solution concentration.

Reverse salt flux is widely used to estimate salt rejection in FO process.[8, 51] Reverse salt flux was measured using 1.0 M NaCl draw solution and pure water as feed solution and exhibited 1.5 g m^{-2} h^{-1}, whereas commercial CTA membrane has a reverse salt flux of around 8.5 g m^{-2} h^{-1}, clearly indicating that GO-polymer membrane achieved much better salt rejection. Furthermore, membrane salt rejection, hereafter defined as FO salt rejection, was calculated from water flux and reverse salt flux based on the equation (3) in the Supplementary Information. Note that although the salt rejection of desalination membranes is mainly obtained by the RO experiment,[7] the salt rejection can be calculated from FO water flux and reverse salt flux to conveniently compare the FO membrane performance. We applied this calculation method to the CTA membrane and obtained a FO salt rejection of 98.2 %, which is slightly lower than 99.3 % measured by the RO experiment.[52] It is obvious that the FO salt rejection is also a better indicator for the membrane performance in the FO processes. Our GO-P61 membrane shows a FO salt rejection of 99.9 %, which is much better than CTA membrane. Moreover, FO performances of GO-polymer membranes remain the same after a few weeks of continuous laboratory tests, demonstrating excellent stability.

To understand the mechanism of its high salt rejection, GO-P61 membrane was analyzed by X-ray diffraction (XRD) to determine the GO interlayer spacing. There are two diffraction peaks in the XRD pattern shown in **Fig. S7**, i.e., one weak peak at 8.5° (d-spacing 1.04 nm) and the other strong peak at 18.0° (d-spacing 0.48 nm). This indicates that the small interlayer spacing (0.48 nm) dominates in the GO-polymer thin film, providing effective rejection of salt ions. Note that without crosslinked polymer network, the GO laminate only shows one

diffraction peak at around 8.5°,[53] and this explains why pure GO membranes have low salt rejection. In our case, the combination of the high hydrophilicity of both GO nanosheets and polymer network and the small interlayer spacing of GO nanosheets fixed by crosslinked polymer network ensures fast water transport and high salt rejection.

Importantly the introduction of highly porous support layer minimizes osmotic pressure drop due to the support layer as illustrated in **Fig. S8**. The main reason of ICP on the FO membrane is due to the high water flux hindrance by the support layer that causes osmotic pressure gradient between the bottom of support layer and the interface with active layer.[54] Therefore, in our study, the highly porous support layer reduced the water flux hindrance and maintained osmotic pressure. It is the mechanically-robust nature of the GO nanosheets polymer composites that serve as a scaffold, and thus enable the formation of an ultrathin GO-polymer thin-film composite layer that allow such a highly porous support to be used.

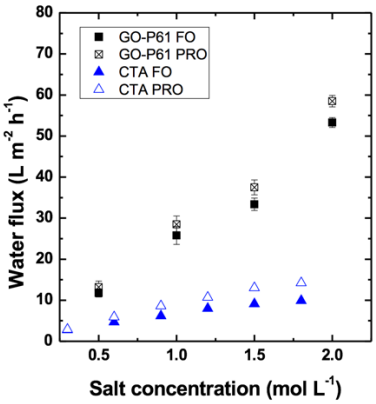

Fig. 5 Water flux of GO-polymer membrane (GO-P61) and CTA membrane in both FO and PRO modes.

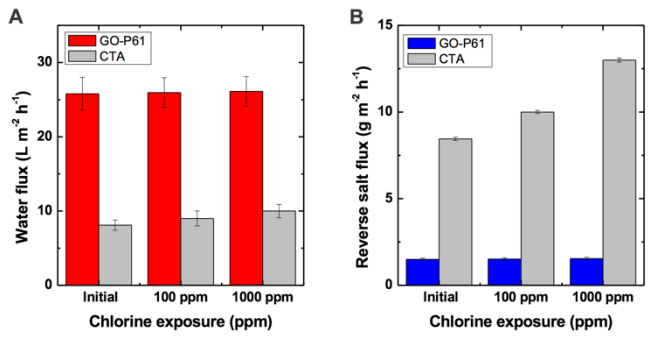

Fig. 6 Chlorine tolerance of GO-polymer (GO-P61) and CTA mem-branes after exposure at 100, and 1,000 ppm for 24 h. Performance changes in (A) water flux and (B) reverse salt flux.

The water flux of the GO-polymer membranes was measured in both FO and PRO modes and compared with that of commercial CTA membranes, with the result shown in **Fig. 5**. The water flux of CTA membrane as a function of the concentration of draw salt solution shows a large difference between FO and PRO modes especially at high salt concentrations. CTA membrane exhibits a similar water flux at the very low salt concentrations, but water flux declines to about 70% at FO mode than that of PRO mode by ICP effects.[50] However in the case of GO-polymer membranes, ICP effects are minimized at FO mode and water flux decreases by only 10% at FO mode even at the high salt concentrations, which can be an advantage for industrial FO processes, given the difficulty of using the membrane in the PRO mode

The GO-polymer membranes produced also have outstanding chlorine tolerance. As shown in **Fig. 6**, after 24 h exposure to 100 ppm and 1,000 ppm chlorine, the water flux and reverse salt flux of the membrane showed negligible change. Note that commercial CTA membranes lost their salt rejection properties after chlorine exposure, resulting in increasing both water flux and reverse salt flux. Only a few ppm of chlorine are used in industrial processes, and our tests using a higher ppm of chlorine thus provide confidence in chlorine resistance of GO-polymer membranes.

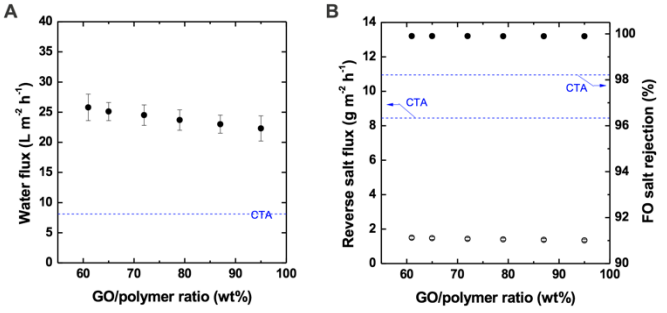

Fig. 7 (A) Water flux and (B) salt rejection properties (black circle: FO salt rejection, white circle: reverse salt flux) of GO-polymer composite membranes as a function of GO-polymer ratio (Feed solution: pure water, draw solution: 1.0 M NaCl).

We also examined the effects of the ratio of GO and polymer on membrane performance. The ratio of GO and polymer in GO-polymer membranes was varied from 61% to 95% of GO by mass, and is summarized in **Table 1**. From SEM observations, there was no significant difference in morphology among samples (**Fig. S9**). The thickness of GO-polymer membranes ranged from 25.9 nm to 39.5 nm, depending on GO content. Water flux and reverse salt flux of GO-polymer membranes with different GO/polymer ratios are shown in **Fig. 7**. Water flux and reverse salt flux were measured using pure water as feed solution and 1.0 M NaCl solution as draw solution. Both water flux and reverse salt flux slightly decreased with increasing GO content; this can be explained by the non-permeable GO nanosheets increasing the resistance of water transport through GO-polymer membranes. GO-P61 membrane (61 wt% GO) exhibited water flux of 25.8 L m^{-2} h^{-1}; when GO content increased to 95 wt% and the water flux of the GO-P95 membrane decreased to 22.3 L m^{-2} h^{-1}. However, in terms of salt rejection, the reverse salt flux and FO salt rejection remained almost unchanged at different GO contents. The overall FO performance of GO-polymer membranes is thus significantly affected by the ratio of GO and

polymer, and this provides a significant flexibility for the membrane fabrication.

Conclusions

We have demonstrated the fabrication of GO entwined by poly(NIPAM-MBA) thin-film composite membranes supported on highly porous Nylon membrane substrate for desalination application. A defect-free, active layer with a very low thickness of less than 40 nm is successfully fabricated by spin-coating and in situ polymerization. The polymer network in the GO-polymer composite enables excellent membrane mechanical stability and processability while maintaining the physical properties of GO nanosheets that facilitate water transport. GO-polymer thin-film composite membrane endures high chlorine exposure at 1,000 ppm for 24 h without noticeable change, demonstrating outstanding chlorine tolerance. Such a defect-free composite membrane has significant advantages for practical FO applications because of the highly porous support layer and a thin coating layer. It is very important that high water flux is maintained for high osmotic pressure differences because the ICP effect is much reduced by the use of highly porous Nylon support layer. Consequently, FO performances in FO and PRO modes are equally remarkable. Integration of GO and polymer network brings both advantages of high water flux and rejection in GO and good processability in polymers, providing a platform material for desalination membranes. Moreover, outstanding water flux and salt separation properties of GO-polymer membranes would lead to energy-efficient water desalination and other applications.

Acknowledgements

This work is supported by the Baosteel-Australia Research and Development Centre (BA13005) and the Australian Re-search Council (Linkage Project No.: LP140100051). The authors acknowledge the staff of Monash Center for Electron Microscopy (MCEM) for their technical assistance with the use of electron microscopes and the Melbourne Centre for Nanofabrication (MCN) in the Victorian Node of the Australian National Fabrication Facility (ANFF) for AFM measurements.

Notes and references

1. P. Bernardo, E. Drioli and G. Golemme, *Ind. Eng. Chem. Res.*, 2009, **48**, 4638-4663.
2. M. A. Shannon, P. W. Bohn, M. Elimelech, J. G. Georgiadis, B. J. Marinas and A. M. Mayes, *Nature*, 2008, **452**, 301-310.
3. M. Mulder, *Basic principles of membrane technology*, Springer Science & Business Media, 1996.
4. J. H. Kim, S. H. Park, M. J. Lee, S. M. Lee, W. H. Lee, K. H. Lee, N. R. Kang, H. J. Jo, J. F. Kim, E. Drioli and Y. M. Lee, *Energy Environ. Sci.*, 2016, **9**, 878-884.
5. M. Elimelech and W. A. Phillip, *Science*, 2011, **333**, 712-717.
6. D. Li, Y. Yan and H. Wang, *Prog. Polymr. Sci.*, 2016, **61**, 104-155.
7. T. Y. Cath, A. E. Childress and M. Elimelech, *J. Membr. Sci.*, 2006, **281**, 70-87.
8. A. P. Straub, A. Deshmukh and M. Elimelech, *Energy Environ. Sci.*, 2016, **9**, 31-48.
9. X. Song, Z. Liu and D. D. Sun, *Energy Environ. Sci.*, 2013, **6**, 1199-1210.
10. G. Z. Ramon, B. J. Feinberg and E. M. V. Hoek, *Energy Environ. Sci.*, 2011, **4**, 4423-4434.
11. Z. Liu, H. Bai, J. Lee and D. D. Sun, *Energy Environ. Sci.*, 2011, **4**, 2582-2585.
12. L. F. Greenlee, D. F. Lawler, B. D. Freeman, B. Marrot and P. Moulin, *Water Res.*, 2009, **43**, 2317-2348.
13. H. B. Park, B. D. Freeman, Z. B. Zhang, M. Sankir and J. E. McGrath, *Angew. Chem. Int. Edit.*, 2008, **47**, 6019-6024.
14. K. L. Cho, A. J. Hill, F. Caruso and S. E. Kentish, *Adv. Mater.*, 2015, **27**, 2791-2796.
15. Y. Zhu, W. Xie, S. Gao, F. Zhang, W. Zhang, Z. Liu and J. Jin, *Small*, 2016, **12**, 5034-5041.
16. H. W. Kim, H. W. Yoon, S.-M. Yoon, B. M. Yoo, B. K. Ahn, Y. H. Cho, H. J. Shin, H. Yang, U. Paik and S. Kwon, *Science*, 2013, **342**, 91-95.
17. R. K. Joshi, P. Carbone, F. C. Wang, V. G. Kravets, Y. Su, I. V. Grigorieva, H. A. Wu, A. K. Geim and R. R. Nair, *Science*, 2014, **343**, 752-754.
18. H. Liu, H. Wang and X. Zhang, *Adv. Mater.*, 2015, **27**, 249-254.
19. F. Perreault, A. F. de Faria and M. Elimelech, *Chem. Soc. Rev.*, 2015, **44**, 5861-5896.
20. J. Liao, Z. Wang, C. Gao, S. Li, Z. Qiao, M. Wang, S. Zhao, X. Xie, J. Wang and S. Wang, *Chem. Sci.*, 2014, **5**, 2843-2849.
21. P. Sun, R. Ma, H. Deng, Z. Song, Z. Zhen, K. Wang, T. Sasaki, Z. Xu and H. Zhu, *Chem. Sci.*, 2016, DOI: 10.1039/C6SC02865A.
22. B. Mi, *Science*, 2014, **343**, 740-742.
23. C.-H. Yang, P.-L. Huang, X.-F. Luo, C.-H. Wang, C. Li, Y.-H. Wu and J.-K. Chang, *ChemSusChem*, 2015, **8**, 1779-1786.
24. Y. Lin, X. Han, C. J. Campbell, J.-W. Kim, B. Zhao, W. Luo, J. Dai, L. Hu and J. W. Connell, *Adv. Funct. Mater.*, 2015, **25**, 2920-2927.
25. Z. Wen, X. Wang, S. Mao, Z. Bo, H. Kim, S. Cui, G. Lu, X. Feng and J. Chen, *Adv. Mater.*, 2012, **24**, 5610-5616.
26. X. Zhao, C. M. Hayner, M. C. Kung and H. H. Kung, *ACS Nano*, 2011, **5**, 8739-8749.
27. Z. Lei, J. Zhang, L. L. Zhang, N. A. Kumar and X. S. Zhao, *Energy Environ. Sci.*, 2016, **9**, 1891-1930.
28. X. Han, M. R. Funk, F. Shen, Y.-C. Chen, Y. Li, C. J. Campbell, J. Dai, X. Yang, J.-W. Kim, Y. Liao, J. W. Connell, V. Barone, Z. Chen, Y. Lin and L. Hu, *ACS Nano*, 2014, **8**, 8255-8265.
29. J.-G. Gai, X.-L. Gong, W.-W. Wang, X. Zhang and W.-L. Kang, *J. Mater. Chem. A*, 2014, **2**, 4023-4028.
30. J. Shen, G. Liu, K. Huang, W. Jin, K.-R. Lee and N. Xu, *Angew. Chem. Int. Edit.*, 2015, **127**, 588-592.
31. Y. Han, Z. Xu and C. Gao, *Adv. Funct. Mater.*, 2013, **23**, 3693-3700.
32. L. Qiu, X. Zhang, W. Yang, Y. Wang, G. P. Simon and D. Li, *Chem. Comm.*, 2011, **47**, 5810-5812.
33. Y. Wang, S. Chen, L. Qiu, K. Wang, H. Wang, G. P. Simon and D. Li, *Adv. Funct. Mater.*, 2015, **25**, 126-133.
34. F. o. Perreault, M. E. Tousley and M. Elimelech, *Environ. Sci. Technol. Lett.*, 2013, **1**, 71-76.
35. W. Choi, J. Choi, J. Bang and J.-H. Lee, *ACS Appl. Mater. Interfaces*, 2013, **5**, 12510-12519.
36. X. Zhang, X. Fan, H. Li and C. Yan, *J. Mater. Chem.*, 2012, **22**, 24081-24091.

37. H. M. Hegab, A. ElMekawy, T. G. Barclay, A. Michelmore, L. Zou, C. P. Saint and M. Ginic-Markovic, *ACS applied materials & interfaces*, 2016, **8**, 17519-17528.
38. M. E. Ali, L. Wang, X. Wang and X. Feng, *Desalination*, 2016, **386**, 67-76.
39. E. Curcio, G. Profio, E. Fontananova, E. Drioli, A. Basile and A. Rastogi, *Membrane technologies for seawater desalination and brackish water treatment*, 2015.
40. K. Xu, B. Feng, C. Zhou and A. Huang, *Chemical Engineering Science*, 2016, **146**, 159-165.
41. X.-L. Xu, F.-W. Lin, Y. Du, X. Zhang, J. Wu and Z.-K. Xu, *ACS applied materials & interfaces*, 2016.
42. L. Shao, X. Cheng, Z. Wang, J. Ma and Z. Guo, *Journal of Membrane Science*, 2014, **452**, 82-89.
43. D. A. Dikin, S. Stankovich, E. J. Zimney, R. D. Piner, G. H. Dommett, G. Evmenenko, S. T. Nguyen and R. S. Ruoff, *Nature*, 2007, **448**, 457-460.
44. W. S. Hummers Jr and R. E. Offeman, *J. Am. Chem. Soc.*, 1958, **80**, 1339-1339.
45. R. Barbey, L. Lavanant, D. Paripovic, N. Schüwer, C. Sugnaux, S. Tugulu and H.-A. Klok, *Chem. Rev.*, 2009, **109**, 5437-5527.
46. K. Zhang, J. Ma, B. Zhang, S. Zhao, Y. Li, Y. Xu, W. Yu and J. Wang, *Mater. Lett.*, 2007, **61**, 949-952.
47. C. Barthet, A. J. Hickey, D. B. Cairns and S. P. Armes, *Adv. Mater.*, 1999, **11**, 408-410.
48. C. D. Easton, A. J. Bullock, G. Gigliobianco, S. L. McArthur and S. MacNeil, *J. Mater. Chem. B*, 2014, **2**, 5558-5568.
49. T. Y. Cath, M. Elimelech, J. R. McCutcheon, R. L. McGinnis, A. Achilli, D. Anastasio, A. R. Brady, A. E. Childress, I. V. Farr and N. T. Hancock, *Desalination*, 2013, **312**, 31-38.
50. S. Zhao, L. Zou and D. Mulcahy, *J. Membr. Sci.*, 2011, **382**, 308-315.
51. W. A. Phillip, J. S. Yong and M. Elimelech, *Environ. Sci. Technol.*, 2010, **44**, 5170-5176.
52. I. L. Alsvik and M.-B. Hägg, *Polymers*, 2013, **5**, 303-327.
53. D. C. Marcano, D. V. Kosynkin, J. M. Berlin, A. Sinitskii, Z. Sun, A. Slesarev, L. B. Alemany, W. Lu and J. M. Tour, *ACS Nano*, 2010, **4**, 4806-4814.
54. X. Song, Z. Liu and D. D. Sun, *Adv. Mater.*, 2011, **23**, 3256-3260.

TOC

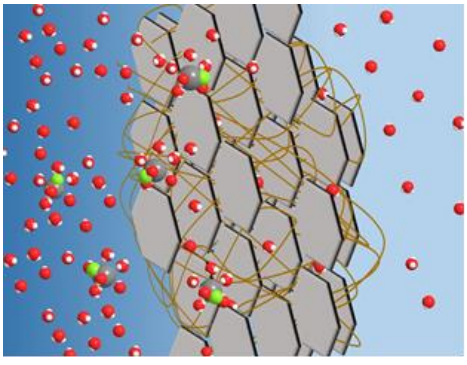

This work demonstrates the successful fabrication of graphene-based thin-film composite membrane by integrating graphene oxide (GO) nanosheets into a highly crosslinked polymer network on a porous polymer substrate. The resulting poly(N-isopropylacrylamide-co-N,N'-methylene-bisacrylamide) entwined GO thin-film composite membrane has a main GO interlayer spacing of 0.48 nm and a GO-polymer thin film of less than 40 nm thick, and shows excellent water flux (25.8 L m^{-1} h^{-1}) and salt rejection (a NaCl rejection of 99.9%), alongside excellent mechanical stability and chlorine tolerance for the forward osmosis process.